

1 **RESPECT THE UNSTABLE: DELAYS AND SATURATION IN**
2 **CONTACT TRACING FOR DISEASE CONTROL ***

3 RICHARD PATES[†], ANDRES FERRAGUT[‡], ELIJAH PIVO[§], PENGCHENG YOU[¶],
4 FERNANDO PAGANINI[‡], AND ENRIQUE MALLADA[¶]

5 **Abstract.** Motivated by the novel coronavirus disease (COVID-19) pandemic, this paper aims
6 to apply Gunter Stein’s cautionary message of *respecting the unstable* to the problem of controlling
7 the spread of an infectious disease. With this goal, we study the effect that delays and capacity
8 constraints in the **test, trace and isolate (TeTrIs)** process have on preventing exponential disease
9 spread. Our analysis highlights the critical importance of speed and scale in the **TeTrIs** process.
10 Precisely, having a delay in the **TeTrIs** process smaller than the doubling time of the disease spread
11 is necessary for achieving acceptable performance. Similarly, limited **TeTrIs** capacity introduces a
12 threshold on the size of an outbreak beyond which the disease spreads almost like the uncontrolled
13 case. Along the way, we provide numerical illustrations to highlight these points.

14 **Key words.** feedback control, stabilization, epidemic spread, COVID-19

15 **AMS subject classifications.** 93D15, 93D09, 93D20, 92D25, 92D30

16 **1. Introduction.** The opening lines of Gunter Stein’s classic paper *Respect the*
17 *Unstable* [24], published 13 years after his inaugural Bode Lecture of the same name,
18 read:

19 “The practical, physical (and sometimes dangerous) consequences of
20 control must be respected, and the underlying principles must be
21 clearly and well taught.”

22 The message to the control engineer and researcher is clear. Not only must the many
23 benefits of feedback be understood (pedagogically, mathematically, and in practice),
24 but also its limitations. The principle of feedback is after all inherently about trade-
25 offs, constrained by conservation laws just as fundamental as any law of physics.
26 Whilst these ‘laws of feedback’ apply to the control of all systems, Gunter Stein gave
27 special attention to unstable systems for three main reasons:

- 28 1. Unstable systems are fundamentally, and quantifiably, more difficult to con-
29 control than stable ones.
- 30 2. Controllers for unstable systems are operationally critical.
- 31 3. Closed-loop systems with unstable components are only locally stable.

32 In this paper we aim to revisit these points from the perspective of designing contact
33 tracing policies to mitigate the spread of disease throughout a population.

34 **1.1. Control of Disease Spread.** The control of disease spread is not the
35 traditional hunting ground of the control engineer, so a degree of caution from our
36 community is perhaps of even greater relevance than normal. That said, controlling
37 the spread of a disease has many of the elements of the most challenging control
38 problems. Accurate models of the spread of a highly infectious disease are at best

*Submitted to the editors Nov. 1st, 2020.

Funding: This work was funded by NSF through grants CAREER 1752362 and TRIPODS 1934979, and Johns Hopkins University Discovery Award.

[†]Lund University, Lund, Sweden. (richard.pates@control.lth.se).

[‡]Universidad ORT, Montevideo, Uruguay, (ferragut@ort.edu.uy, paganini@ort.edu.uy)

[§]Massachusetts Institute of Technology, Boston, MA USA, (epivo@mit.edu)

[¶]Johns Hopkins University, Baltimore MD, USA (pcyou@jhu.edu, mallada@jhu.edu)

39 controversial, but certainly unstable (at least in a population with high susceptibility
 40 to the disease). The mechanisms for identifying infectious members of the population
 41 may be subject to significant delays and inaccuracies, compromising the quality of the
 42 available information for performing feedback. And finally, the options for mitigating
 43 the spread can be blunt, unpredictable, and subject to severe capacity constraints.

44 Since emerging in late 2019, the novel coronavirus disease (COVID-19) pandemic
 45 has made abundantly clear the effect that these challenges have in mitigating disease
 46 spread. At the time of writing, there have been nearly 45 million documented cases of
 47 COVID-19 [7]. Without a vaccine, the primary public health tools available to limit
 48 the spread are non-pharmaceutical interventions (NPIs) such as social distancing and
 49 contact tracing [11]. Many NPIs can be understood in terms of feedback control,
 50 and as such abide by the fundamental ‘laws of feedback’ that Gunter Stein referred
 51 to. This work aims to develop an analysis that illustrates the impact that these
 52 limitations, placing a particular emphasis on the role of delays and saturation. We
 53 focus on contact tracing as it exhibits several of the features described before.

54 **1.2. Contact Tracing.** Contact tracing is the process of testing, tracing and
 55 isolating people known to have been in close proximity with infected individuals. All
 56 three of these steps are essential, so for this reason contact tracing is also referred
 57 to by the acronym **TeTrIs**. This intervention can disrupt chains of infection to slow
 58 and potentially end the spread of an infectious disease. It has been employed in the
 59 control of sexually transmitted diseases [6, 12, 19], in limiting the severe acute respira-
 60 tory syndrome (SARS) epidemic [5] and at an unprecedented scale in the COVID-19
 61 pandemic [23, 1].

62 The ways that **TeTrIs** is carried out differs from region to region and are rapidly
 63 evolving. Regardless of the specifics, two key characteristics contribute to the success
 64 of **TeTrIs**. The first is the delay between the moment an individual becomes infected
 65 and the moment that individual becomes isolated from the rest of the population. A
 66 larger delay allows the infected individual to infect more people. The second is the
 67 capacity of the **TeTrIs** program. We think of this capacity as the number of active
 68 cases the **TeTrIs** program can process at once without the delay growing significantly.
 69 These characteristics are determined by the structure of the **TeTrIs** program. But
 70 more practically, achieving sufficient performance in these characteristics must be
 71 used to determine the structure of the **TeTrIs** program. Thus, in this paper we seek
 72 to characterize sufficient delays and capacity of a **TeTrIs** program to successfully
 73 control the spread of an infectious disease.

74 These affects of these characteristics have been studied in the past. Many works
 75 analyze the impacts of contact tracing using computer simulations [18, 10]. Math-
 76 ematical analysis of **TeTrIs** has typically relied on two methodologies. In the first,
 77 an ordinary differential equation (ODE) models spread over a certain fixed contact
 78 graph [9, 14]. In the second, the impact of **TeTrIs** is modeled as a branching process
 79 [21, 20].

80 **1.3. Contributions of this Work.** In this work, we take a control theoretic
 81 perspective on the impacts of delays and saturation. These two phenomenon have
 82 been widely studied in the control systems field. We provide two rules of thumb for
 83 the requisite speed and capacity of a **TeTrIs** system. First, we show that short delays
 84 may suffice to overwhelm a **TeTrIs** system by analyzing their impact on the system
 85 sensitivity function. For infectious diseases analogous to COVID-19, the optimistic
 86 allowable delay to control their initial outbreak is approximately 1 day. Another
 87 implication of the analysis points to the importance of effective isolation. If we fail

88 to isolate two thirds of the cases, such a system is not stabilising even without delay.
 89 Second, we model the contact tracing process and show that the saturation of its
 90 limited capacity may disable an otherwise efficacious TeTrIs system. With saturation,
 91 we identify a threshold behavior of disease spread that implies stability regions beyond
 92 capacity and potentially significant degradation of performance.

93 The paper is structured as follows. First, we discuss the effects of delay on the
 94 efficacy contact tracing. We introduce contact tracing as a feedback loop on the classic
 95 SIR model. We derive an upper bound on allowable delay to control disease spread in
 96 this setting. Then, we generalize this analysis from the SIR model to LTI systems and
 97 nonlinear systems with an exponential unstable mode. Second, we discuss the effects
 98 of saturation on the efficacy contact tracing. We introduce two compartmental models
 99 that respectively capture the contact tracing efforts devoted to infected and uninfected
 100 population and introduce the saturation effects of tracing capacity. Reduced stability
 101 regions are observed based on a nonlinear threshold analysis.

102 **Notation.** Transfer functions of **linear-time-invariant (LTI)** systems will be de-
 103 noted with bold face letters. For example $\mathbf{G}(s) = 1/(s + 1)$ is the transfer function
 104 from u to x for the system $\frac{dx}{dt} = -x + u$, and $\mathbf{G}(s) = \exp(-sT)$ the transfer function
 105 for the delay $x(t) = u(t - T)$. The set of all proper real rational transfer functions,
 106 i.e. functions on the form

$$107 \quad \mathbf{G}(s) = \frac{a_0 s^n + a_1 s^{n-1} + \dots + a_n}{s^n + b_1 s^{n-1} + \dots + b_n}, a_i \in \mathbb{R}, b_k \in \mathbb{R}$$

108 will be denoted by \mathcal{R} . The H-infinity norm of a transfer function \mathbf{G} is defined as

$$109 \quad \|\mathbf{G}\|_\infty := \sup \{ |\mathbf{G}(s)| : s \in \mathbb{C}, \text{Re}(s) > 0 \}.$$

110 The H-infinity norm is a central notion in the robust performance of control systems,
 111 see for example [8, §2] for an introduction.

112 **2. Contact tracing: The Need for Speed.** The basic rationale behind TeTrIs
 113 is simple. Disease spreads through the contact between infectious and susceptible
 114 members of a population. So by rapidly isolating infectious individual as soon as
 115 they are detected, as well as everyone they've recently contacted (who may now be
 116 infectious themselves), it may be possible to shut off all the routes of spread, and stop
 117 an outbreak in its tracks. But how accurate does the testing need to be to ensure
 118 that enough cases are traced? And how fast must the system be to halt an outbreak
 119 before it becomes an epidemic?

120 In this section we will explore these questions from the control-theoretic perspec-
 121 tive, with a particular focus on feedback based fundamental limitations. TeTrIs is a
 122 feedback process, in which infectious people are isolated in response to measurements
 123 about a population. Therefore TeTrIs is subject to conservation laws and performance
 124 limitations (see [24, 2] for an introduction). We will discuss the consequences of these,
 125 placing a particular focus on the following inequality:

$$126 \quad (2.1) \quad \|\mathbf{S}\|_\infty \geq 2^{\frac{T_{\text{delay}}}{T_{\text{doubling}}}}.$$

127 The precise meanings of all these terms will be made clear when it is derived in
 128 **Subsection 2.2**, but here \mathbf{S} is the sensitivity function (in the usual control theoretic
 129 sense), T_{doubling} the doubling time of the unstable process¹, and T_{delay} the sum of

¹Here $T_{\text{doubling}} := \frac{\ln 2}{p}$, where $p > 0$ is the location of the unstable pole.

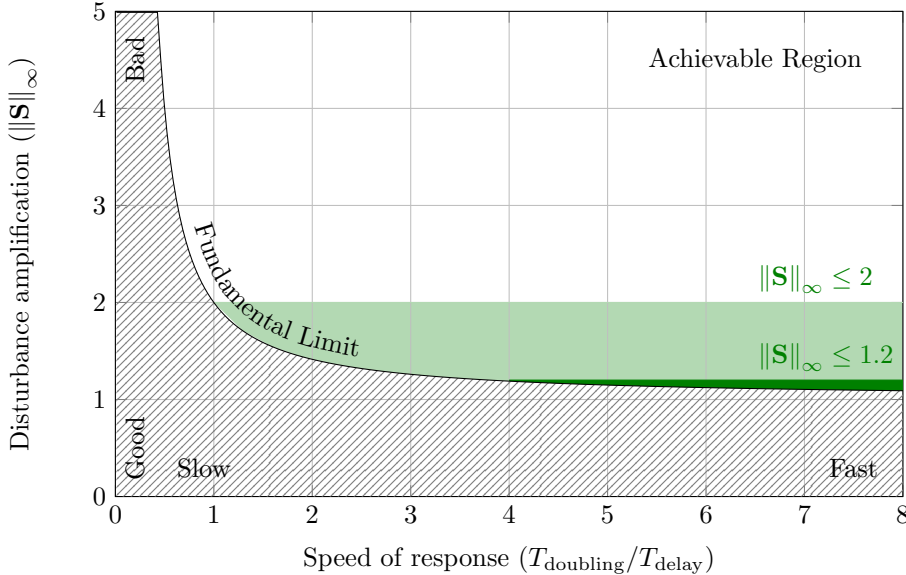


FIG. 1. Trade-off between disturbance amplification and time delay when controlling an unstable system. Typically $\|\mathbf{S}\|_\infty$ less than 1.2–2 is necessary for good performance.

130 delays in the feedback loop. This inequality imposes a fundamental limit on the size
 131 of the sensitivity function, and shows that when very unstable processes (smaller
 132 doubling times) are controlled with large delays, the sensitivity function will always
 133 be large. This is illustrated in Figure 1. Since the sensitivity function determines how
 134 disturbances are amplified and attenuated, (2.1) demonstrates that in such systems,
 135 bad performance is inevitable. Indeed the conventional wisdom is that a value of
 136 $\|\mathbf{S}\|_\infty$ less than 1.2–2 is a prerequisite for acceptable performance (see e.g. [3, 8]).
 137 The size of $\|\mathbf{S}\|_\infty$ is also intimately related to many other measures of performance
 138 and robustness, such as gain and phase margins [3, §7.2].

139 Equation (2.1) gives the implication

$$140 \quad T_{\text{delay}} > T_{\text{doubling}} \log_2 k_{\text{perf}} \implies \|\mathbf{S}\|_\infty > k_{\text{perf}}.$$

141 The consequences of this inequality is quite striking in the context of controlling dis-
 142 ease spread using TeTrIs. For example it shows that given a disease with a doubling
 143 time of 8 days, if the delays between becoming infectious and being isolated are greater
 144 than 2 days, then $\|\mathbf{S}\|_\infty > 1.2$ (picking the more conservative target might be advis-
 145 able when trying to control a highly uncertain system such as disease spread). This
 146 bound holds even under extremely optimistic assumptions about the implementation
 147 of contact tracing. Specific implementations can certainly be worse!

148 What makes the bound useful is that it provides direct insight into our original
 149 questions. For example if we set a target of $\|\mathbf{S}\|_\infty \leq 1.2$, the system set up to conduct
 150 contact tracing must be at least four times faster than doubling time of the disease:

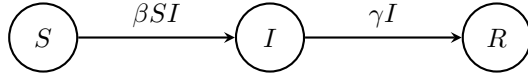
$$151 \quad \|\mathbf{S}\|_\infty \leq 1.2 \implies T_{\text{delay}} \leq T_{\text{doubling}}.$$

152 Slower implementations are guaranteed to fail this objective, and as a result be more
 153 vulnerable to disturbances (e.g. failing to identify an infectious person could result

154 in a large number of new infections). It is interesting to note that the same rule of
 155 thumb based on more ad-hoc arguments can be found in [4, §III.B-4)]. Inequalities
 156 such as (2.1) provide further evidence for the necessity of a fast TeTrIs system.

157 **2.1. Understanding the Issue.** In this section we will demonstrate the funda-
 158 mental limitation discussed above from the perspective of a simple model of contact
 159 tracing. This will allow us to put these abstract ideas in a more concrete setting, so
 160 as to better understand them. Studying a simple model will also allow us to derive
 161 specialised analysis tools along the way that can provide additional insight. In what
 162 follows we will first outline a simple SIR-based model for contact tracing, before il-
 163 lustrating the fundamental limitations through simulations and additional theoretical
 164 tools.

165 **2.1.1. An SIR-based Model for Disease Control with TeTrIs.** The so
 166 called SIR model is one of the simplest and most widely used models of disease spread
 167 [16]. It is centred around three compartments - $S(t)$, $I(t)$ and $R(t)$ - which specify the
 168 proportion of the population that are susceptible, infectious, and recovered at time t .
 169 So if $S(0) = 1$, then at time $t = 0$ the entire population is susceptible to the disease,
 170 or if $R(1) = 0.5$ then half the population has recovered (or died) at time $t = 1$. The
 171 population shifts between these compartments over time according to two rates, which
 172 model the effect of the infectious population mixing with the susceptible population
 173 and transferring the disease, and the infectious population recovering, respectively.
 174 This can be visualised on a graph with a node for each compartment, and a directed
 175 edge specifying the transition rates between them:



176 Here β is a mixing parameter, specifying the average number of ‘significant’ (those
 177 that could result in the transmission of the disease) interactions that each individual
 178 has per unit time. Each infectious person then has an average of βS such events
 179 with the susceptible population, resulting in βSI new infections per unit time. The
 180 second rate is justified by saying that on average it takes $1/\gamma$ units of time for an
 181 infectious person to recover, which corresponds to members of the I compartment
 182 being transferred to the R compartment with rate γI .

184 When written as a set of differential-algebraic equations, the SIR model is

185 (2.2)
$$\frac{d}{dt} \begin{bmatrix} S \\ I \\ R \end{bmatrix} = \begin{bmatrix} -1 \\ 1 \\ 0 \end{bmatrix} \beta SI + \begin{bmatrix} 0 \\ -1 \\ 1 \end{bmatrix} \gamma I, \quad 1 = S + I + R.$$

186 Of central importance in the study of the SIR model (and disease spread in general)
 187 is the so called basic reproduction number R_0 . R_0 is defined to be the number of
 188 secondary infections caused by a single primary infection in a population in which
 189 everyone is susceptible to the disease. Consequently if $R_0 > 1$ a small outbreak will
 190 spread, whereas if $R_0 < 1$ it will not. For the SIR model, $R_0 = \beta/\gamma$. This is closely
 191 related to notions of stability and doubling times. For the SIR model

192 (2.3)
$$T_{\text{doubling}} = \frac{\ln 2}{\beta - \gamma} = \frac{\ln 2/\beta}{1 - 1/R_0}.$$

193 The SIR model describes the process of disease spread, but not the impact of TeTrIs.
 194 To model this, we first split the infectious population into two groups Q and I_{mix} ,

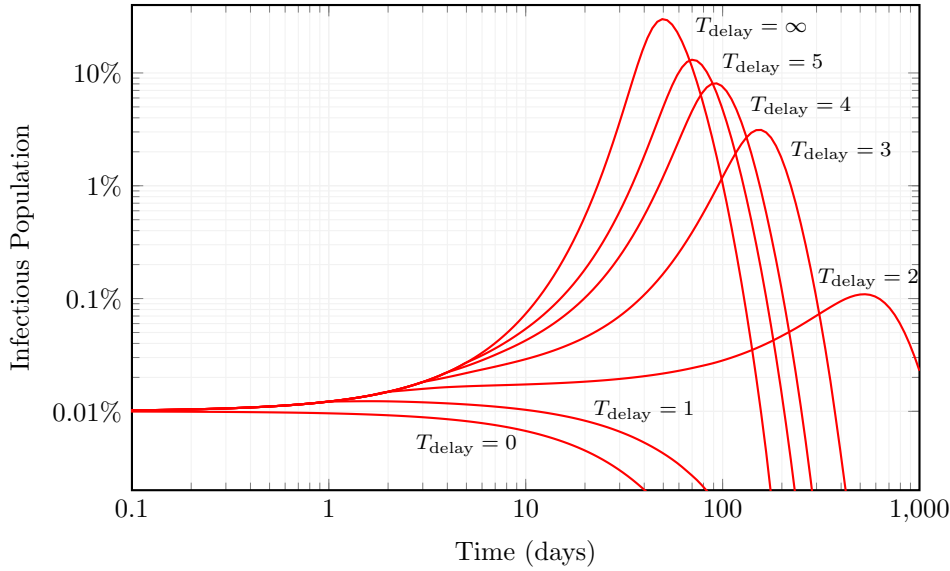
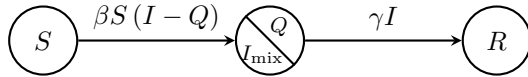


FIG. 2. Simulation of (2.4) and (2.5) for a range of values of T_{delay} .

195 where Q corresponds to the subpopulation that has been quarantined, and I_{mix} the
 196 remainder of the infectious population. We can incorporate the effect of quarantining,
 197 by modifying the rate between the susceptible and infectious population as shown
 198 below. The rationale here is that after taking quarantining into account there should
 199 be $\beta S I_{\text{mix}}$ new infections per unit time, and that $I_{\text{mix}} = I - Q$.



200
 201 The effect of this change is to slightly modify the original SIR equation in (2.2):

202 (2.4)
$$\frac{d}{dt} \begin{bmatrix} S \\ I \\ R \end{bmatrix} = \begin{bmatrix} -1 \\ 1 \\ 0 \end{bmatrix} \beta S (I - Q) + \begin{bmatrix} 0 \\ -1 \\ 1 \end{bmatrix} \gamma I, \quad 1 = S + I + R.$$

203 All that remains is to close the loop, and specify how the number of people who are
 204 quarantined at time t depends on the contact tracing. For simplicity, we propose to
 205 model this process through the equation

206 (2.5)
$$Q(t) = \alpha e^{-\gamma T_{\text{delay}}} I(t - T_{\text{delay}}),$$

207 where $1 \geq \alpha \geq 0$ and $T_{\text{delay}} \geq 0$. In words this equation says that we are able to
 208 test, trace and isolate a proportion α of those that were infectious T_{delay} days ago².
 209 Together (2.4) and (2.5) constitute a simple model for understanding how TeTrIs can
 210 be used to control disease spread.

211 **2.1.2. Analysis of the Simple Model.** Before performing a theoretical analy-
 212 sis of the model, it is instructive to run some simulations. The evolution of the

²We need to include the proportional constant $e^{-\gamma T_{\text{delay}}}$ since over those T_{delay} days, $(1 - e^{-\gamma T_{\text{delay}}})$ of those that were infectious will have gone on to recover.

213 infectious population after an outbreak affecting 0.01% of the population is shown in
 214 [Figure 2](#) for a range of different values of the time delay. The simulation parameters
 215 for this figure are:

- 216 • $\alpha = 0.8$, meaning that 80% of cases are tested, traced and isolated.
- 217 • $\gamma = 0.1$, meaning the disease has an average recovery time of 10 days.
- 218 • $\beta = 0.3$, giving the disease a basic reproduction number of 3.

219 The first thing to note is that if the delay is short, the outbreak is contained and
 220 no epidemic ensues. It is also interesting to see the degradation in behaviour as the
 221 delay increases. By the time T_{delay} is 5 days, an epidemic not dissimilar to that
 222 without [TeTrIs](#) occurs. Even more strikingly though is that by the time T_{delay} is just
 223 2 days, the initial outbreak sees a tenfold increase before it is brought under control.
 224 This relatively short delay has seemingly brought [TeTrIs](#) to the verge of instability.
 225 When you consider that there may be several simultaneous outbreaks, or capacity
 226 constraints on how many people that can be tested-and-traced, it is clear that short
 227 delays may already be enough overwhelm a [TeTrIs](#) system.

228 A natural first question is, “*Are these results in line with the fundamental limita-*
 229 *tion discussed at the beginning of this section?*”. A simple calculation shows that at
 230 the start of the outbreak, the doubling time of the disease equals

$$231 \quad T_{\text{doubling}} = \frac{\ln 2}{\beta - \gamma} \approx 3.5 \text{ days.}$$

232 Therefore to achieve $\|\mathbf{S}\|_{\infty} \leq 1.2$, it is necessary that $T_{\text{delay}} \leq 0.9$ days. This seems
 233 to be in good agreement with the simulation, where the case with a one day delay
 234 is well controlled, with a rapid decline in performance soon after. In fact, given the
 235 simple nature of the model in [\(2.4\)](#) and [\(2.5\)](#) a more detailed analysis is possible.
 236 The following theorem characterises the stability of the linearisation of the model
 237 about the disease free equilibrium in terms of the system parameters. An intuitive
 238 explanation of this stability criterion is given at the end of the section.

239 **THEOREM 2.1.** *The linearisation of the model in [\(2.4\)](#) and [\(2.5\)](#) is stable about*
 240 *the point $(I, R, Q) = (0, 0, 0)$ if and only if*

$$241 \quad (2.6) \quad T_{\text{delay}} < \frac{1}{\gamma} \ln \left(\frac{\alpha\beta}{\beta - \gamma} \right).$$

242 *Proof.* See [Appendix A](#). □

243 In order to interpret the meaning of [Theorem 2.1](#) it helps to rearrange the bound
 244 a little:

$$245 \quad \gamma T_{\text{delay}} < \ln \left(\frac{\alpha\beta}{\beta - \gamma} \right) = \ln \left(\frac{\alpha}{1 - 1/R_0} \right).$$

246 The specific trade-off between parameters and delay implied by the above is shown in
 247 [Figure 3](#). This figure can be used to quickly assess the amount of delay that can be
 248 tolerated before instability occurs. For example, in the simulations we used a model
 249 with $R_0 = 3$ and $\gamma = 0.1$, with feedback parameter $\alpha = 0.8$. Therefore from the figure
 250 we see that we require

$$251 \quad T_{\text{delay}}\gamma < 0.18, \implies T_{\text{delay}} < 1.8 \text{ days}$$

252 for the policy to be stabilising. This captures precisely the behaviour we saw in the
 253 simulation, where $T_{\text{delay}} = 2$ seemed to be right on the cusp of instability. We also

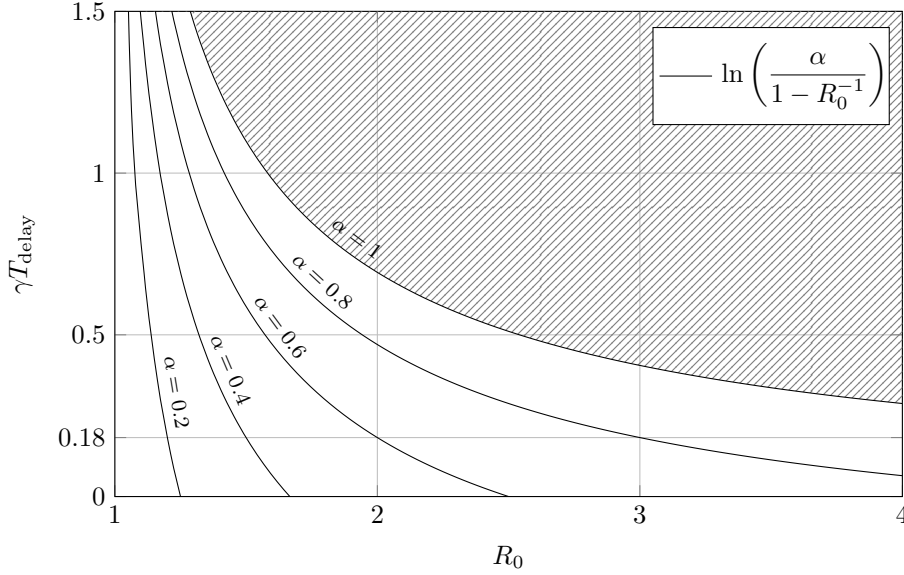


FIG. 3. Illustration of the stability boundary in [Theorem 2.1](#). The model of *TeTrIs* is stabilising if and only if $(R_0, \gamma T_{\text{delay}})$ lies below the corresponding α curve. For example, if $\alpha = 0.8$ and $R_0 = 3$, the model is stable if and only if $\gamma T_{\text{delay}} < 0.18$

254 see the importance of tracing enough cases. By the time $\alpha < 1 - R_0^{-1} = 2/3$, that is
 255 we only detect and isolate at most 66% of the cases, the policy isn't even stabilising
 256 with $T_{\text{delay}} = 0$.

257 The stability criterion in [Theorem 2.1](#) also has a nice interpretation though the
 258 effective reproduction number R . Suppose that α in [\(2.5\)](#) is the probability that
 259 an infectious individual is detected and isolated. The amount of time T that each
 260 infectious person is mixing with the susceptible population is then a random variable

$$261 \quad T = \begin{cases} T_r & \text{w.p. } 1 - \alpha \\ \min \{T_{\text{delay}}, T_r\} & \text{w.p. } \alpha. \end{cases}$$

262 In the above $T_r \sim \text{Exp}(\gamma)$ is the time it takes the given person to recover from the
 263 disease. Therefore the expected time that each infectious person is in the mix is given
 264 by

$$265 \quad \begin{aligned} \mathbb{E}[T] &= (1 - \alpha) \mathbb{E}[T_r] + \alpha \mathbb{E}[\min \{T_{\text{delay}}, T_r\}] = (1 - \alpha) \frac{1}{\gamma} + \alpha \int_0^{T_{\text{delay}}} \exp(-\gamma s) ds \\ &= \frac{1}{\gamma} (1 - \alpha \exp(-\gamma T_{\text{delay}})). \end{aligned}$$

266 The effective reproduction number is then the expected number of secondary infections
 267 generated by an individual:

$$268 \quad R = \beta \mathbb{E}[T] = \frac{\beta}{\gamma} (1 - \alpha \exp(-\gamma T_{\text{delay}})) = R_0 (1 - \alpha \exp(-\gamma T_{\text{delay}})).$$

269 The condition that $R < 1$, which would correspond to an outbreak dying out, is thus

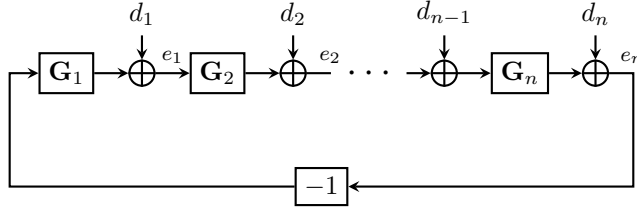


FIG. 4. Feedback interconnection in (2.7).

270 equivalent to

271
$$1 > R_0 (1 - \alpha \exp(-\gamma T_{\text{delay}})) \iff T_{\text{delay}} < \frac{1}{\gamma} \ln \left(\frac{\alpha}{1 - R_0^{-1}} \right),$$

272 which is precisely the stability condition from [Theorem 2.1](#).

273 **2.2. Fundamental Limitations.** A natural concern with the results from [Sub-](#)
 274 [section 2.1.2](#) is that they are seemingly based on a set of highly contentious modelling
 275 assumptions. For example, why use SIR model to capture the effect of disease spread
 276 in (2.4), rather than the SEIR model or indeed any of the other more complex com-
 277 partmental variants? What about other models for [TeTrIs](#)? Will the same conclusions
 278 hold if we use something more realistic than (2.5)? In this section we will demonstrate
 279 that the limitations we observed through [Theorem 2.1](#) and the simulations of (2.4)
 280 and (2.5) are really a consequence of the interplay between instability and delay.

281 The main result of this section is to derive the inequality (2.1). For simplicity
 282 we will stick to the [LTI](#) case, though we will show in [Appendix B](#) that a natural
 283 analogue of (2.1) holds in the nonlinear case also. To this end, consider the feedback
 284 interconnection of n subsystems described by

285 (2.7)
$$\begin{aligned} \hat{e}_i &= \mathbf{G}_i \hat{e}_{i-1} + \hat{d}_i, \quad i \in \{1, \dots, n\} \\ \hat{e}_0 &= -\hat{e}_n. \end{aligned}$$

286 In the above the variables \hat{d}_i and \hat{e}_i denote the Laplace transforms of a set of scalar
 287 disturbances and error signals, and \mathbf{G}_i the transfer function of the i -th subsystem.
 288 The basic set up is illustrated in [Figure 4](#). This is a general framework for describing
 289 feedback systems, and many models for the control of a disease using [TeTrIs](#) can be
 290 put in this framework. For example, after linearisation about the point $(I, R, Q) =$
 291 $(0, 0, 0)$, the model in (2.4) and (2.5) can be captured by setting $n = 2$, and

292 (2.8)
$$\mathbf{G}_1(s) = \frac{\beta}{s - (\beta - \gamma)}, \quad \mathbf{G}_2(s) = \alpha \exp(-sT_{\text{delay}}).$$

293 Variants with, for example, more complicated compartmental models of disease spread
 294 can be similarly handled by substituting in the corresponding transfer function for
 295 \mathbf{G}_1 .

296 The advantage of the abstract formulation in (2.8) is that it allows general prop-
 297 erties of feedback interconnections to be studied for entire classes of model. When
 298 studying the properties of this feedback interconnection, the central objects are the
 299 sensitivity functions. These are the transfer functions from d_i to e_i , which we denote
 300 as \mathbf{S}_i . In the [LTI](#) case, the sensitivity functions are all equal to each other and given

301 by

$$302 \quad (2.9) \quad \mathbf{S}_i = \frac{1}{1 + \mathbf{G}_1 \mathbf{G}_2 \cdots \mathbf{G}_n} =: \mathbf{S}, \quad i \in \{1, \dots, n\}.$$

303 These functions determine how the internal signals \hat{e}_i depend on the external
 304 disturbances \hat{d}_i . Hence the size of \mathbf{S} determines how disturbances are attenuated.
 305 Indeed every single closed loop transfer function in (2.8) contains \mathbf{S} (for example the
 306 transfer function from \hat{d}_1 to \hat{e}_3 is given by $\mathbf{G}_3 \mathbf{G}_2 \mathbf{S}$). Given its central importance to
 307 the process of feedback, the sensitivity function has been extensively studied both in
 308 theory and in practice. Indeed the requirement that the size of $\|\mathbf{S}\|_\infty$ be less than
 309 1.2–2 is widely used, and is arguably of more importance than the criteria on the gain
 310 margin and phase margin³ [3, §7.2].

311 The following theorem shows that when the feedback loop contains a system with
 312 an unstable pole p and a time delay of T_{delay} , $\|\mathbf{S}\|_\infty \geq \exp(pT_{\text{delay}})$. This places
 313 a fundamental limit on the size of the sensitivity function. Surprisingly this result
 314 doesn't seem to be known (for example the lower bound $\|\mathbf{S}\|_\infty \geq \exp(pT_{\text{delay}}) - 1$ is
 315 presented in [3, §14.3, Table 14.1]), though the existence of such a bound is certainly
 316 implicit in the work on sensitivity optimisation from the 1980s [17, 13]. We give a
 317 simple proof based on the maximum modulus principle.

318 THEOREM 2.2. *If $\mathbf{L} = \frac{\exp(-sT_{\text{delay}})}{s-p} \mathbf{H}$, where $T_{\text{delay}} > 0, p > 0$ and $\mathbf{H} \in \mathcal{R}$, then*

$$319 \quad \left\| \frac{1}{1 + \mathbf{L}} \right\|_\infty \geq \exp(pT_{\text{delay}}).$$

320 *Proof.* Let $a > 1$, and note that the Möbius transform $f(z) = (1 - az)/(a - z)$
 321 maps the closed unit disc into the closed unit disc. This implies that given any transfer
 322 function \mathbf{G} , we have the equivalence

$$323 \quad \|\mathbf{G}\|_\infty \leq 1 \iff \|f(\mathbf{G})\|_\infty \leq 1.$$

324 Therefore $\|1/(1 + \mathbf{L})\|_\infty \leq a$ if and only if

$$325 \quad 1 \geq \left\| f\left(\frac{1}{a} \frac{1}{1 + \mathbf{L}}\right) \right\|_\infty = \left\| \frac{a\mathbf{L}}{a^2\mathbf{L} + a^2 - 1} \right\|_\infty,$$

$$= \left\| \frac{a\mathbf{H} \exp(-sT_{\text{delay}})}{a^2\mathbf{H} \exp(-sT_{\text{delay}}) + (s-p)(a^2 - 1)} \right\|_\infty.$$

326 Now recall that given any transfer function \mathbf{G} , $\|\mathbf{G} \exp(-sT_{\text{delay}})\|_\infty = \|\mathbf{G}\|_\infty$ (delay-
 327 ing the input to a transfer function doesn't affect its norm). Therefore

$$328 \quad \left\| \frac{a\mathbf{H} \exp(-sT_{\text{delay}})}{a^2\mathbf{H} \exp(-sT_{\text{delay}}) + (s-p)(a^2 - 1)} \right\|_\infty = \left\| \frac{a\mathbf{H}}{a^2\mathbf{H} \exp(-sT_{\text{delay}}) + (s-p)(a^2 - 1)} \right\|_\infty$$

$$\geq \frac{1}{a \exp(-pT_{\text{delay}})},$$

³Indeed it can be shown that [3, §7.2]

$$\text{gain margin} \geq \frac{\|\mathbf{S}\|_\infty}{\|\mathbf{S}\|_\infty - 1}, \quad \text{phase margin} \geq 2 \arcsin\left(\frac{1}{2\|\mathbf{S}\|_\infty}\right),$$

whereas no guarantees in the converse direction hold (positive gain and phase margins only guarantee that $\|\mathbf{S}\|_\infty < \infty$).

329 where the inequality follows from the maximum modulus principle applied at the
 330 point $s = p$ (see e.g. [8, §6.2]). This demonstrates that $\|1/(1 + \mathbf{L})\|_\infty \leq a$ only if
 331 $a \geq \exp(pT_{\text{delay}})$ as required. \square

332 It is readily verified that this bound is equivalent to the inequality presented
 333 earlier in (2.1) by substituting in the relationship between p and T_{doubling} . That is
 334 setting $p = \ln(2)/T_{\text{doubling}}$ shows that

$$335 \quad \|\mathbf{S}\|_\infty \geq \exp(pT_{\text{delay}}) = 2^{\frac{T_{\text{delay}}}{T_{\text{doubling}}}}.$$

336 **Theorem 2.2** shows that if the transfer function $\mathbf{G}_1\mathbf{G}_2 \cdots \mathbf{G}_n$ (typically referred
 337 to as the return ratio) can be written on the form

$$338 \quad (2.10) \quad \mathbf{G}_1\mathbf{G}_2 \cdots \mathbf{G}_n = \frac{\exp(-sT_{\text{delay}})}{s - p}\mathbf{H},$$

339 where \mathbf{H} is any transfer function in \mathcal{R} , then $\|\mathbf{S}\|_\infty \geq \exp(pT_{\text{delay}})$. We therefore
 340 see from (2.8) that **Theorem 2.2** applies to our simple model for disease control with
 341 **TeTrIs** (set $\mathbf{H} = \alpha\beta$). However the true power of **Theorem 2.2** is that it holds for
 342 any feedback interconnection on the form of (2.7) that satisfies (2.10). This means
 343 that the same fundamental limits on performance hold even if we replace our simple
 344 model of disease spread from (2.4) with a general compartmental model which predicts
 345 an initial period of exponential spread of the disease (if there is no spread, **TeTrIs**
 346 is not really necessary anyway). To see this, suppose that the linearisation of our
 347 compartmental model of choice can be written on the general form⁴:

$$348 \quad (2.11) \quad \frac{dx}{dt} = Ax + BQ, \quad I = Cx.$$

349 If the model predicts a period of exponential spread of the disease, then the A matrix
 350 will have an eigenvalue $p > 0$. Provided this mode is observable and controllable
 351 (which would also be necessary for there to be any chance of controlling it through
 352 **TeTrIs**), the transfer function associated with (2.11) will have a pole at p . That is

$$353 \quad \hat{I} = \frac{1}{s - p}\mathbf{M}\hat{Q}.$$

354 Assuming the same model for **TeTrIs** we can now write the linearisation of the
 355 feedback interconnection of (2.5) and (2.11) in the framework of (2.7) by setting
 356 $\mathbf{G}_1 = 1/(s - p)\mathbf{M}$, and leaving $\mathbf{G}_2 = \alpha \exp(-sT_{\text{delay}})$. The transfer functions in this
 357 interconnection also satisfy (2.10), and so the same fundamental limit holds. In fact
 358 it will continue to hold even if we use more complex models for **TeTrIs**, provided they
 359 still include a total time delay of T_{delay} . We conclude the section with some final
 360 remarks on **Theorem 2.2**.

361 *Remark 2.3.* The bound from **Theorem 2.2** also applies to the complementary
 362 sensitivity function. That is, under the conditions of **Theorem 2.2**, $\|\mathbf{L}/(1 + \mathbf{L})\|_\infty \geq$
 363 $\exp pT_{\text{delay}}$.

⁴This is the general form of the linearisation of a compartmental model

$$\frac{dx}{dt} = f(x, Q), \quad I = g(x).$$

It may seem restrictive that g doesn't depend on Q . However if it did, this would mean the effect of quarantining someone would instantly affect whether or not they are infectious, which is rather implausible.

364 *Remark 2.4.* [Theorem 2.2](#) continues to hold in the nonlinear setting under the
 365 assumption that the feedback interconnection in question has a linearisation. This
 366 essentially follows from the fact that the induced \mathcal{L}_2 -norm of a nonlinear system
 367 (the natural generalisation of the H-infinity norm) is always greater than the induced
 368 \mathcal{L}_2 -norm of its linearisation. This effectively shows that by considering the nonlinear
 369 effects in more realistic models, performance (as measured using sensitivity functions)
 370 can only get worse. This makes it all the more important to aim for performance
 371 requirements on the conservative end (i.e. $\|\mathbf{S}\|_\infty \leq 1.2$ rather than $\|\mathbf{S}\|_\infty \leq 2$),
 372 necessitating a speedier response. This is discussed in [Appendix B](#).

373 **2.3. Discussion.** The purpose of this section has been to expose fundamental
 374 limits in epidemic control that arise from the combination of two factors: the natural
 375 open loop instability of the system, and the existence of delays in the feedback loop.
 376 Some of our results were stated in general form, but the main motivating example
 377 is the stabilization and regulation of an epidemic by means of testing, tracing and
 378 isolation of infections. The bounds derived apply to *any* control strategy of this kind,
 379 and can be summarized in "the need for speed": if the delays involved in identifying,
 380 testing and isolating cases are not very tight, the success of the entire approach is in
 381 jeopardy.

382 There are other strategies for an epidemic control, which are also subject to
 383 fundamental limits of this kind. The most commonly deployed one is *social distancing*
 384 of the entire population. In the context of the classical SIR models, this means making
 385 the parameter β itself a control variable, attempting to stabilize the dynamics at a
 386 nonzero number of infections, compatible with the capacity of the healthcare system.
 387 Of course, a model of social behavior that would cover the control of β is not easy
 388 to obtain, and will not be pursued here. We remark, nonetheless, that for instance a
 389 strategy of ordering a lockdown when infections hit a certain threshold is also subject
 390 to time delays (due to disease latency times) which will compromise performance.

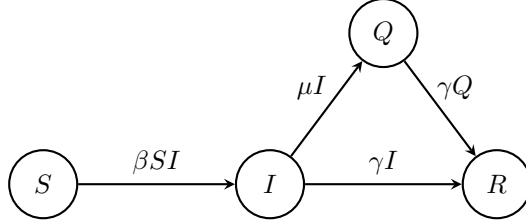
391 Staying within the realm of contact tracing based control, there is another fun-
 392 damental limit that will be analyzed in the following section.

393 **3. Track-and-trace: The Need for Scale.** The analysis of the preceding
 394 section set the focus on the effect feedback *delays* in limiting the performance of the
 395 [TeTrIs](#) strategy for epidemic control. Here we will address a different limitation of the
 396 control strategy that manifests in the presence of disturbances. That is, the above
 397 control strategy relies on scarce resources: the availability of technology and trained
 398 personnel for taking samples and laboratory testing, for the proactive tracking down
 399 of potential infections, and for ensuring appropriate quarantine.

400 These resources are usually orders of magnitude smaller than the full scale of
 401 the population, and thus often saturate in a widespread epidemic such as COVID-
 402 19. The question we wish to address is the characterization of these limitations in
 403 mathematical models for the epidemic under [TeTrIs](#)-based control. To accommodate
 404 the nonlinear effect of saturation in a tractable way, for this analysis we will simplify
 405 the delay-to-quarantine model to a finite dimensional dynamics instead of a pure
 406 delay. This alternative is natural in the context of compartmental models: rather
 407 than assume that the [TeTrIs](#) process takes a fixed amount of time to remove infected
 408 people, we assume a rate of removal is given; this can be seen as the macroscopic
 409 aggregate of the random times involved in the contract tracing process.

410 **3.1. A Model for Contact Tracing.** We thus introduce a compartmental
 411 model that incorporates as a *state* the number of people in quarantine Q , in addition

412 to the the standard susceptible (S), infected (I) and removed (R) populations. We
 413 assume that people in quarantine effectively isolate and thus are no longer producing
 414 new infections.



415
 416 The TeTrIs control strategy is modeled as follows: Infected people are individually
 417 tracked, tested and isolated at a rate μ , meaning that on average, we need a time $1/\mu$
 418 to effectively put these people into quarantine.

419 Under these assumptions, the dynamics become:

420 (3.1)
$$\frac{d}{dt} \begin{bmatrix} S \\ I \\ Q \\ R \end{bmatrix} = \begin{bmatrix} -1 \\ 1 \\ 0 \\ 0 \end{bmatrix} \beta SI + \begin{bmatrix} 0 \\ -1 \\ 1 \\ 0 \end{bmatrix} \mu I + \begin{bmatrix} 0 \\ -1 \\ 0 \\ 1 \end{bmatrix} \gamma I + \begin{bmatrix} 0 \\ 0 \\ -1 \\ 1 \end{bmatrix} \gamma Q.$$

421 This model was already proposed in [22] and its analysis is simple, since quaran-
 422 tined people can be considered as “early recoveries”. More formally, if we consider the
 423 dynamics in $\tilde{S} = S, \tilde{I} = I, \tilde{R} = Q + R$, then the model becomes a simple SIR model
 424 with recovery rate $\gamma + \mu$ and therefore the critical reproduction rate parameter is:

425 (3.2)
$$R_\mu := \frac{\beta}{\gamma + \mu}.$$

426 In the model without quarantine, the open loop critical rates is $R_0 = \beta/\gamma$ (cor-
 427 responding to the case $\mu = 0$). The net effect of contact tracing is to reduce the
 428 reproduction rate: $R_\mu < R_0$. In particular, if the contact tracing rate $\mu \rightarrow 0$ (contact
 429 tracing is extremely slow), things go by as if contact tracing is not operating. If con-
 430 tact tracing is extremely fast ($\mu \rightarrow \infty$), it can stabilize any open loop transmission
 431 rate.

432 In fact, the above analysis gives a first rule of thumb to determine the contact
 433 tracing speed. That is, provided that the open loop system is unstable ($R_0 > 1$), we
 434 need:

435 (3.3)
$$\frac{1}{\mu} < \frac{1}{\beta - \gamma},$$

436 i.e., the average isolation time must be controlled. Eq. (3.3) can be compared with
 437 (2.6), the main difference stems from the fact that here we are continuously isolating
 438 people after a random delay, instead of a fixed one. As an example, if we fix the
 439 average recovery time in $1/\gamma = 10$ days and $R_0 = 3$ ($\beta = 0.3$), the average time to
 440 isolate is bounded by 5 days.

441 While this family of quarantining models is well known, we would like to analyze
 442 the effect of *saturating* the contact tracing capability. To this end, consider that there
 443 is a maximum fraction of the population K that can be tested, tracked, and isolated
 444 simultaneously. This can be due to a limit in the total test processing capability, the
 445 number of contact tracing agents that are deployed or any combination thereof.

446 In such a scenario, if the number of infected people is low, then the quarantining
 447 rate should be μI , since every infected person is being tracked (equivalently there
 448 exists idle tracking and testing capacity). However, if the number of infected people
 449 is high ($I > K$), then the quarantining rate should be μK because of the saturation
 450 of the control capabilities.

451 Under these assumptions, the dynamics become:

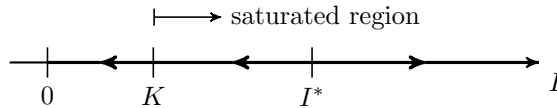
$$452 \quad (3.4) \quad \frac{d}{dt} \begin{bmatrix} S \\ I \\ Q \\ R \end{bmatrix} = \begin{bmatrix} -1 \\ 1 \\ 0 \\ 0 \end{bmatrix} \beta SI + \begin{bmatrix} 0 \\ -1 \\ 1 \\ 0 \end{bmatrix} \mu \min\{K, I\} + \begin{bmatrix} 0 \\ -1 \\ 0 \\ 1 \end{bmatrix} \gamma I + \begin{bmatrix} 0 \\ 0 \\ -1 \\ 1 \end{bmatrix} \gamma Q.$$

453 Note that if $K \geq 1$ in (3.4), we recover the first model.

454 **3.2. Understanding the Issue.** To highlight the issues introduced by this sat-
 455 uration, we first analyze the dynamics (3.4) under the assumption that $S \approx 1$ (i.e. at
 456 the beginning of the epidemic). In that case, the important part of the dynamics is
 457 the evolution of infected people, which becomes autonomous:

$$458 \quad (3.5) \quad \frac{d}{dt} I = \beta I - \gamma I - \mu \min\{K, I\}.$$

459 The above differential equation is extremely simple to analyze. However it yields
 460 an important insight into the effect of saturation in this kind of dynamics. Consider
 461 the case where $R_0 > 1$, i.e. the system is open loop unstable, but $R_\mu < 1$, meaning
 462 that the system can be stabilized by an “infinite” contact tracing capability, as in
 463 (3.1). Then the phase diagram becomes:



464

465 The new unstable equilibrium that emerges in the approximate dynamics can be
 466 readily computed by imposing $dI/dt = 0$ in (3.5) to yield:

$$467 \quad (3.6) \quad I^* = \frac{\mu K}{\beta - \gamma}.$$

468 The appearance of this new equilibrium means that the saturation of contact
 469 tracing measures leads to a threshold behavior in the number of infected people,
 470 a phenomenon already observed in several countries that have lost track of disease
 471 spread [15]. Of course, the value I^* is not an equilibrium of the full non-linear dy-
 472 namics (3.4), but it should operate as a threshold value. We revisit this more formally
 473 below.

474 In addition, using that $R_\mu < 1$, we have $\mu > \beta - \gamma$ and thus $I^* > K$. This means
 475 that the stability region is larger than the saturation point of the contact tracing
 476 capability. One way to interpret the threshold is to rearrange (3.6) in the following
 477 manner:

$$478 \quad (3.7) \quad K = \left(\frac{\beta}{\mu} - \frac{\gamma}{\mu} \right) I^*.$$

479 Here the factor $\frac{\beta}{\mu} - \frac{\gamma}{\mu}$ acts as a reproduction number: it can be interpreted as the
 480 number of “children” of a single infected individual generated until it is traced, minus

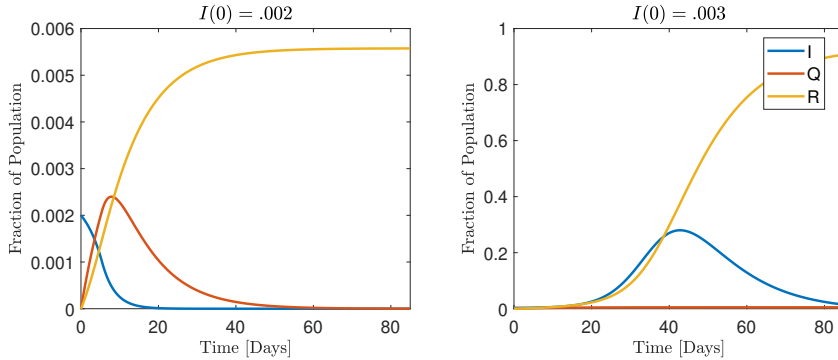


FIG. 5. Simulation of the system in (3.4) with $I(0) = 2 \times 10^{-3} < I^*$ and $I(0) = 3 \times 10^{-3} > I^*$. Note the different scales in the y-axis.

481 the ones that recover in that same period. If the total number of new infections
 482 generated by a pool I of infected people is larger than the tracing capacity, then the
 483 disease will spread in the long run.

484 **Example.** To demonstrate the validity of the approximation $S \approx 1$ at the begin-
 485 ning of the epidemic, consider the following scenario: let $\gamma = 1/10$, i.e. recovery time
 486 around 10 days and $R_0 = 3$ ($\beta = 0.3$) so the system is open loop unstable. Assume
 487 that we need two days on average to test, trace and isolate people, which amounts to
 488 a choice of $\mu = 1/2$. In that case $I^* = \frac{\mu}{\beta - \gamma} K = 2.5K$, that is every unit of tracing
 489 capability can deal with up to 2.5 simultaneous infections without crossing the thresh-
 490 old. Let us simulate the system for an initial condition with $S \approx 1$. In particular
 491 we choose $K = 10^{-3}$, meaning that 1 in 1000 people can be tracked simultaneously.
 492 With this choice of K , $I^* = 2.5 \times 10^{-3}$ and we choose $I(0)$ slightly below or above
 493 I^* . Results are shown in Fig. 5. We can see that the simulated (nonlinear) system
 494 indeed enters the exponential phase immediately after reaching the threshold.

495 The above analysis, albeit simplistic, illustrates the effects of local non-linearities
 496 in the stability behavior of the epidemics, namely that a stable region appears around
 497 the extinction equilibrium, but instability can be reinstated if the number of infected
 498 people grows large, overwhelming the control capabilities. We now analyze this further
 499 in the complete dynamics (3.4), and then extend the framework to consider the case
 500 where the tracing effort is in part spent on contacts that do not become infected.

501 **3.3. Nonlinear Analysis.** To understand the effect of the saturation without
 502 approximating $S \approx 1$, it is of use to first understand the behavior of $S(t)$. Since,
 503 by (3.4), $\frac{d}{dt} S \leq 0$, $S(t)$ is a decreasing function of time. This allows to derive the
 504 following monotonicity property for $I(t)$.

505 **PROPOSITION 3.1** (Monotonicity of $I(t)$ under (3.4)). Consider the dynamics
 506 (3.4). Then the following property holds

507 (3.8)
$$\frac{d}{dt} I(t_0) < 0 \implies \frac{d}{dt} I(t) < 0, \quad \forall t \geq t_0.$$

508 *Proof.* Without loss of generality we assume $I(t_0) > 0$. We first consider the
 509 case $I(t_0) \leq K$. In this case, it follows from (3.4) that $S(t_0) < 1/R_\mu$. This is the
 510 standard scenario where the amount of susceptible people is not enough to sustain
 511 the epidemic, thus we expect $\frac{d}{dt} I(t) < 0$ for all $t > t_0$.

512 Indeed, if we assume by contradiction that there is a time t_1 such that $\frac{d}{dt}I(t_1) = 0$
 513 then we get

$$514 \quad 0 = \frac{d}{dt}I(t_1) = (\beta S(t_1) - \gamma - \mu)I(t_1) \implies S(t_1) = \frac{1}{R_\mu} > S(t_0),$$

515 which contradicts the fact that $S(t)$ is decreasing in time.

516 The analysis for the case $I(t_0) \geq K$ follows a similar reasoning. Indeed, by
 517 considering the saturated version of (3.4), i.e.,

$$518 \quad (3.9) \quad \frac{d}{dt}I = \beta SI - \gamma I - \mu K,$$

519 we get that $\frac{d}{dt}I(t_0) < 0$ implies

$$520 \quad (3.10) \quad (\beta S(t_0) - \gamma)I(t_0) < \mu K.$$

522 Thus, assuming again by contradiction the existence of t_1 , being the first time $\frac{d}{dt}I(t) =$
 523 0 for $t > t_0$, we obtain

$$524 \quad (3.11) \quad (\beta S(t_0) - \gamma)I(t_0) < \mu K = (\beta S(t_1) - \gamma)I(t_1) \leq (\beta S(t_0) - \gamma)I(t_1)$$

526 where the first inequality follows from $\frac{d}{dt}I(t_0) < 0$ and the second from the mono-
 527 tonicity of $S(t)$. It follows then that $I(t_1) > I(t_0)$, and therefore

$$528 \quad 0 < I(t_1) - I(t_0) = \int_{t_0}^{t_1} \frac{d}{dt}I(t)dt < 0,$$

529 where the last inequality holds by the definition of t_1 . Thus, such a time t_1 cannot
 530 exist. \square

531 The preceding proposition illustrates the critical role of the nullcline $\frac{d}{dt}I = 0$
 532 in (3.4) in understanding the threshold behavior in the nonlinear case. To simplify
 533 exposition and further understand the role of the nullcline, we consider only the most
 534 relevant case when $R_\mu < 1$ and $R_0 > 1$, as before.

535 In this case, the nullcline is fully within the saturated region, and Proposition 3.1
 536 leads to the simple condition

$$537 \quad (3.12) \quad I \leq \tilde{I}(S) := \frac{\mu K}{\beta S - \gamma} = \frac{\mu K}{\beta(S - \frac{1}{R_0})}.$$

538 for the disease to dissipate without a major outbreak. Indeed, for the number of
 539 infectious people to increase, $\frac{d}{dt}I(t)$ must be positive, thus violating (3.12).

540 A few remarks are in order. First, the threshold is only valid for the range
 541 $0 \leq \tilde{I}(S) \leq 1$. Outside such range, the disease dies out. In particular, $0 \leq \tilde{I}(S)$ leads
 542 to the already known $S \leq 1/R_0$ condition, and $\tilde{I}(S) \geq 1 \geq I$ guarantees $\frac{d}{dt}I < 0$ for
 543 all I . Second, the nonlinear threshold $\tilde{I}(S)$, is a decreasing function of S (see Figure
 544 6), which implies that the most conservative bound is obtained at $S = 1$, which leads
 545 to

$$546 \quad \tilde{I}(S) = \frac{\mu K}{\beta S - \gamma} \geq \frac{\mu K}{\beta - \gamma} = I^* > K,$$

547 where the last inequality follows from our assumption $R_\mu < 1$. Thus, the analysis
 548 of the previous section leads to a *lower bound* on the critical threshold which, as
 549 expected, is quite accurate when $S \approx 1$.

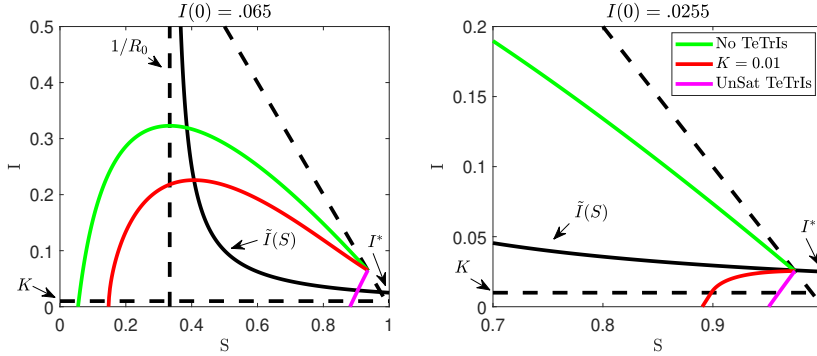


FIG. 6. S - I region of the phase plane. Trajectories for uncontrolled evolution (green), unsaturated *TeTrIs* (purple), and *TeTrIs* with $K = 0.01$ (red) are presented for two initial conditions. On the left, $I(0)$ is above the nullcline and the pandemic spreads. On the right, $I^* < I(0) < \tilde{I}(S(0))$ and the pandemic is contained successfully. The $\tilde{I}(S)$ nullcline (solid black) thus acts as a threshold between successful and unsuccessful *TeTrIs*.

550 **Example.** Consider again the set of parameters $\beta = 0.3$, $\gamma = 1/10$ and $\mu = 1/2$.
 551 As mentioned before, since in this case $R_\mu < 1 < R_0$, $\tilde{I}(S) \geq I^* > K$ holds for all S .
 552 Fig. 6 consider the case of $K = 0.01$ (red) and compare its trajectory on the (S, I)
 553 plane with two additional cases, the unsaturated dynamics (*UnSatTeTrIs*, purple)
 554 and the regular dynamics with no track-and-trace (*NoTeTrIs*, red). On the left, an
 555 initial condition $I(0) = 0.65$, $S(0) = 1 - I(0)$, with $I(0)$ above the threshold $\tilde{I}(S)$ (solid
 556 black) is considered. On the right, a similar setting but with $I(0) = 0.0255$ between
 557 $\tilde{I}(S(0)) = \tilde{I}(.974) = .026$ and $I^* = .025$ is considered. This therefore validates the
 558 very slight conservativeness in the I^* threshold.

559 **3.4. Modeling the Tracing of Uninfected Contacts.** One thing the pre-
 560 ceding models do not capture is that the resources of a contact tracing system are
 561 also invariably used to test and trace people that have been in contact with infected
 562 individuals, but *have not* developed the infection. As we analyze in this section,
 563 the stability region obtained by *TeTrIs* control policy will be reduced because of this
 564 phenomenon.

565 Consider the following compartmental model for the epidemic spread. As usual
 566 I denotes the infected population at a given time. These infected individuals have
 567 multiple contacts which generate secondary infections at rate β , but also have other
 568 contacts, say at rate β_1 , which do *not* generate infection. Since this classification
 569 can only be ascertained by testing, the *TeTrIs* capability is in part spent on these
 570 non-infected contacts. We will denote the population of *potential infections* by P ,
 571 and separate it from the rest of the susceptible population which for which we use the
 572 variable S .

573 For our model, we choose $\beta_1 = \nu\beta$. Here ν can be thought as the “odds ratio” that
 574 a contacted individual does not develop the infection. If $\nu = 0$ all potential contacts
 575 are infected and the model operates as before, but typically $\nu > 0$ meaning that not all
 576 contacts are infected. In particular, in Uruguay where we have access to fine grained
 577 data, its value is around $\nu = 10$, meaning that for each infected individual, 10 more
 578 people should be tracked.

579 The open loop model given below carries out the classification of susceptible

580 individuals into the P and S categories, before incorporating contact tracing:

$$581 \quad (3.13) \quad \frac{d}{dt} \begin{bmatrix} S \\ P \\ I \\ R \end{bmatrix} = \begin{bmatrix} -1 - \nu \\ \nu \\ 1 \\ 0 \end{bmatrix} \beta IS + \begin{bmatrix} 0 \\ -1 \\ 1 \\ 0 \end{bmatrix} \beta IP + \begin{bmatrix} 0 \\ 0 \\ -1 \\ 1 \end{bmatrix} \gamma I.$$

582 Of course, if we combined both categories of susceptibles into one class $\tilde{S} = S + P$,
 583 the model reduces to a classical SIR model with infection rate β and recovery rate
 584 γ . Thus the reproduction number for the model in (3.13) is given as before by:

$$585 \quad R_0 = \frac{\beta}{\gamma}.$$

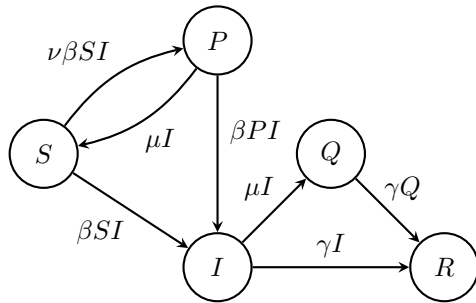
586 Consider now that the contact tracing effort u is split between u_P and u_I , mean-
 587 ing that the tracking is performed over the whole potentially infected population.
 588 Those that are tracked and are infected are isolated, the others are simply ‘‘cleared’’
 589 and return to the normal susceptible class. Adding as before a state variable for
 590 quarantined population we obtain the model:

$$591 \quad (3.14) \quad \frac{d}{dt} \begin{bmatrix} S \\ P \\ I \\ Q \\ R \end{bmatrix} = \begin{bmatrix} -1 - \nu \\ \nu \\ 1 \\ 0 \\ 0 \end{bmatrix} \beta IS + \begin{bmatrix} 0 \\ -1 \\ 1 \\ 0 \\ 0 \end{bmatrix} \beta IP + \begin{bmatrix} 1 \\ -1 \\ 0 \\ 0 \\ 0 \end{bmatrix} u_P + \begin{bmatrix} 0 \\ 0 \\ -1 \\ 1 \\ 0 \end{bmatrix} u_I + \begin{bmatrix} 0 \\ 0 \\ -1 \\ 0 \\ 1 \end{bmatrix} \gamma I + \begin{bmatrix} 0 \\ 0 \\ 0 \\ -1 \\ 1 \end{bmatrix} \gamma Q.$$

592 Following the analysis in the previous sections, in the case where there is no limit
 593 to the tracing capabilities, we can assume that:

$$594 \quad (3.15) \quad u_P = \mu P, \quad u_I = \mu I$$

595 where $1/\mu$ is the average time to trace and test one individual, either potential or
 596 infected.



597 Substituting this control law in eq. (3.14), we can easily observe that, since there
 598 is no coupling between u_P and u_I , the model reduces to the contact tracing and
 599 quarantining model of Section 3.1. Namely, the state $\tilde{S} = S + P$, $\tilde{I} = I$, $\tilde{Q} = Q$ and
 600 $\tilde{R} = R$ follows exactly the dynamics in (3.1). In particular, the reproduction rate for
 601 a given value of μ is the same as in (3.2):
 602

$$603 \quad (3.16) \quad R_\mu = \frac{\beta}{\mu + \gamma}.$$

604 Again with sufficiently fast contact tracing, one can cope with any transmission rate.

605 The interesting case, however, is when contact tracing is limited by the total
 606 number of trackers or simultaneous tests that can be performed. Since these tests are
 607 performed *before* knowing if a person is a potential infection or a infected individual,
 608 the coupling between u_P and u_I becomes

609 (3.17)
$$u_P + u_I \leq \mu K.$$

610 In particular, if we assume that the effort is equally split between all $P + I$
 611 potentially infected individuals, then:

612 (3.18)
$$u_P(P, I) = \mu \frac{P}{P + I} \min\{P + I, K\} = \mu P \min\left\{1, \frac{K}{P + I}\right\},$$

613 (3.19)
$$u_I(P, I) = \mu \frac{I}{P + I} \min\{P + I, K\} = \mu I \min\left\{1, \frac{K}{P + I}\right\}.$$

 614

615 Note that $u_P + u_I = \mu \min\{K, P + I\}$ and thus satisfies (3.17). Also when I and P
 616 are near zero, the feedback law reduces to (3.15).

617 **3.5. Threshold Analysis.** In comparison with (3.4), a full non linear analysis
 618 in this case is more involved. Therefore, we resort to the strategy of analyzing the
 619 behavior of the saturated policy around the disease free equilibrium where $S \approx 1$.
 620 In this setting, $P \ll 1$ and $I \ll 1$ so the product term IP can be disregarded.⁵
 621 Substituting this condition and the control law (3.18) in (3.14), the dynamics becomes
 622 autonomous in P and I with equation:

623 (3.20)
$$\frac{d}{dt} \begin{bmatrix} P \\ I \end{bmatrix} = \begin{bmatrix} 0 & \nu\beta \\ 0 & \beta - \gamma \end{bmatrix} \begin{bmatrix} P \\ I \end{bmatrix} - \mu \min\left\{1, \frac{K}{P + I}\right\} \begin{bmatrix} P \\ I \end{bmatrix}.$$

624 We have the following:

625 **PROPOSITION 3.2.** *Under the condition $R_0 > 1$ (uncontrolled open loop) and*
 626 *$R_\mu < 1$, the dynamics in (3.20) have a locally asymptotically stable disease free equi-*
 627 *librium $P = I = 0$, and a further unstable equilibrium emerges at:*

628 (3.21)
$$P^* = \frac{\nu\beta}{((1 + \nu)\beta - \gamma)(\beta - \gamma)} \mu K, \quad I^* = \frac{1}{(1 + \nu)\beta - \gamma} \mu K.$$

629 *Proof.* We begin by analyzing the disease free case, which is readily verified it is
 630 an equilibrium after substitution in (3.20). The Jacobian matrix in this case retains
 631 a diagonal term $-\mu$ since the saturation is not in effect near the origin. Thus the
 632 Jacobian is:

633
$$J_1 = \begin{bmatrix} -\mu & \nu\beta \\ 0 & \beta - \gamma - \mu \end{bmatrix}.$$

634 The Jacobian has two eigenvalues, $-\mu < 0$ and $\beta - \gamma - \mu$ which is negative because
 635 of the assumption that $R_\mu < 1$, hence the equilibrium is locally stable.

636 To find the second equilibrium, we assume that the saturation is active and impose
 637 equilibrium in (3.20):

638
$$\begin{bmatrix} 0 & \nu\beta \\ 0 & \beta - \gamma \end{bmatrix} \begin{bmatrix} P^* \\ I^* \end{bmatrix} - \mu \frac{K}{P^* + I^*} \begin{bmatrix} P^* \\ I^* \end{bmatrix} = \begin{bmatrix} 0 \\ 0 \end{bmatrix}$$

⁵This is equivalent to considering that every potential contact only arises from a single infected interaction

639 After some algebra one arrives at the expressions in (3.21) for P^* and I^* .
 640 Furthermore:

$$641 \quad (3.22) \quad P^* + I^* = \frac{\mu}{\beta - \gamma} K > K$$

642 under the hypothesis that $\mu > \nu\beta - \gamma \Leftrightarrow R_\mu < 1$. Hence, for any testing rate that
 643 stabilizes under infinite contact tracing assumptions, one gets an unstable equilibrium
 644 when the saturation comes into play. Moreover, note that the total number being
 645 tracked in this new equilibrium coincides with the threshold (3.6).

646 That this equilibrium is indeed unstable can be seen analyzing its Jacobian ma-
 647 trix, which is just:

$$648 \quad J_2 = \begin{bmatrix} 0 & \nu\beta \\ 0 & \beta - \gamma \end{bmatrix}$$

649 which corresponds to the open loop model that has a positive eigenvalue $\beta - \gamma > 0$
 650 under the assumption $R_0 > 1$. \square

651 As a final remark, note that the equilibrium (3.21) verifies:

$$652 \quad (3.23) \quad \frac{P^*}{I^*} = \frac{\nu\beta}{\beta - \gamma} = \frac{R_0}{R_0 - 1}\nu.$$

653 This supports the intuitive observation that, when ν is large, most of the contact
 654 tracing effort is spent only in the potential contacts, reducing the stability margin.
 655 Below we analyze this in a numerical example.

656 **Example.** To depict the behavior of the dynamics (3.20), we choose as before
 657 $\gamma = 1/10$ (10 days average recovery time) and $\beta = 3\gamma$, yielding $R_0 = 3$. The ratio ν
 658 is taken as $\nu = 10$ as observed in some cases, consistent with current measurements
 659 in the real epidemiological scenario in Uruguay, where approximately 10 contacts are
 660 traced per infected individual, generating only one new infection.

661 If we assume that $K = 10^{-3}$, meaning that 1 in 1000 people can be tracked and
 662 tested simultaneously, then the unstable equilibrium occurs at:

$$663 \quad P^* + I^* = 2.5 \times 10^{-3},$$

664 but with a lower number of infections, namely:

$$665 \quad P^* = 2.34 \times 10^{-3}, \quad I^* = 0.16 \times 10^{-3}.$$

666 Observe that these parameters are also consistent with the numerical example
 667 in Section 3.1, where the stability threshold was at $I = 2.5 \times 10^{-3}$. Now that the
 668 contact tracing is burdened with potential contacts the stability region diminishes in
 669 consequence.

670 The phase plot is depicted in Figure 7. In particular, starting from an initial
 671 condition $I(0) = 0.5 \times 10^{-3}$ (which would be clearly stable in (3.4)) and $P(0) = 0$, the
 672 system enters the exponential phase due to the secondary contacts that burden the
 673 contact tracing capabilities. In particular, in Fig. 8 we can observe that at the peak
 674 70% of the population becomes a potential contact simultaneously, and the susceptible
 675 people go quickly to 0, meaning that the whole population has become into contact
 676 with an infected individual, clearly overwhelming the tracking and testing capabilities.

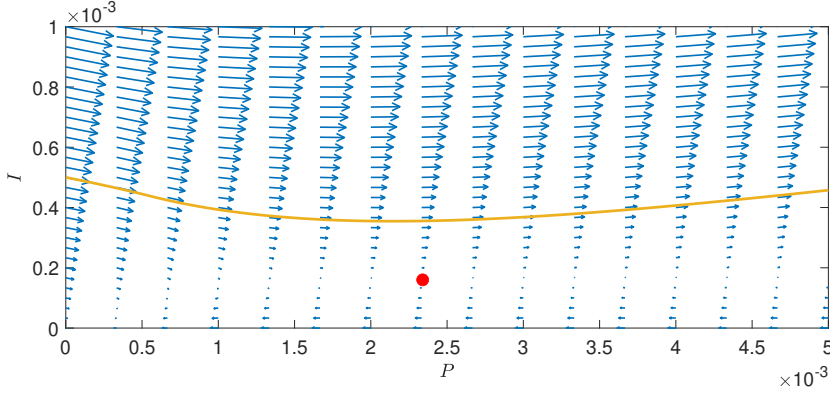


FIG. 7. Phase diagram of (3.20) and unstable equilibrium point of the approximate dynamics. We superimpose the solution of the nonlinear version depicted in Fig. 8.

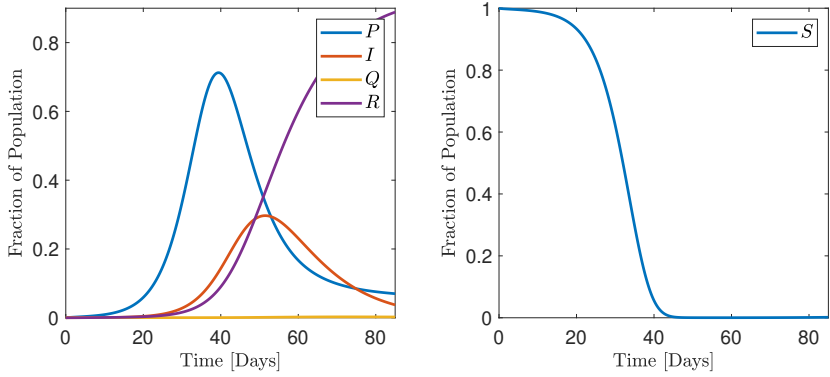


FIG. 8. Unstable trajectories of the saturated system with limited contact tracing.

677 **3.6. Discussion.** To conclude this section, let us recap the main results derived.
 678 The first result is that, whenever there is a cap on the contact tracing capability, a
 679 threshold behavior develops in the dynamics. This emphasizes the *need for scale*,
 680 summarized succinctly in eq. (3.6) and its nonlinear counterpart (3.12). Whenever
 681 the infected number grows, the testing and tracing capacity should grow linearly
 682 with the number of infections in order to avoid saturation. On the other hand, the
 683 system can work in the saturated regime without becoming overwhelmed, but once
 684 the threshold is crossed the epidemic will spread.

685 The second result is that this stability margin is greatly compromised by the fact
 686 that testing and tracing capacity is burdened with the need of following contacts that
 687 do not become infected. This is summarized in eqs. (3.22) and (3.23), that evidence
 688 how saturation comes into play due to the total number of contacts, and that this
 689 total number is dominated by potential contacts.

690 **4. Conclusions.** This work presents a cautionary message of the fundamental
 691 limits involved in preventing disease propagation during an epidemic. Our results
 692 highlight the particularly dangerous combination of instability and non-linearity, in-
 693 trinsic of the disease spread process (our plant), together with delays and capacity

694 constraints, intrinsic of the TeTrIs process (our actuator), that makes the disease con-
 695 trol problem fundamentally challenging. It is important to notice that some of our
 696 quantitative predictions, are up to a certain extent pessimistic, as we only consider
 697 one method for disease spread prevention, i.e., TeTrIs . Clearly, complementing such
 698 process with other control mechanisms, such as social distancing, using masks, etc.,
 699 can improve the effectiveness and robustness of the disease spread mitigation efforts.
 700 Nevertheless, irrespective of the methods used, we believe that the need for speed and
 701 scale are at its core necessary for effective disease prevention.

702

REFERENCES

- 703 [1] *Contact tracing in the context of covid-19*, May 2020, [https://www.who.int/publications/i/](https://www.who.int/publications/i/item/contact-tracing-in-the-context-of-covid-19)
 704 [item/contact-tracing-in-the-context-of-covid-19](https://www.who.int/publications/i/item/contact-tracing-in-the-context-of-covid-19). Accessed: 2020-10-30.
- 705 [2] K. J. ÅSTRÖM, *Limitations on control system performance*, European Journal of Control, 6
 706 (2000), pp. 2–20.
- 707 [3] K. J. ÅSTRÖM AND R. M. MURRAY, *Feedback systems: an introduction for scientists and*
 708 *engineers*, Princeton university press, 2 ed., 2010.
- 709 [4] F. CASELLA, *Can the covid-19 epidemic be controlled on the basis of daily test reports?*, IEEE
 710 Control Systems Letters, 5 (2020), pp. 1079–1084.
- 711 [5] M. CHAN-YEUNG AND R.-H. XU, *Sars: epidemiology*, Respirology, 8 (2003), pp. S9–S14.
- 712 [6] J. CLARKE, *Contact tracing for chlamydia: data on effectiveness*, International journal of STD
 713 & AIDS, 9 (1998), pp. 187–191.
- 714 [7] E. DONG, H. DU, AND L. GARDNER, *An interactive web-based dashboard to track covid-19 in*
 715 *real time*, The Lancet infectious diseases, 20 (2020), pp. 533–534.
- 716 [8] J. C. DOYLE, B. A. FRANCIS, AND A. R. TANNENBAUM, *Feedback control theory*, Macmillan
 717 Publishing Co, 1992.
- 718 [9] K. T. EAMES AND M. J. KEELING, *Contact tracing and disease control*, Proceedings of the
 719 Royal Society of London. Series B: Biological Sciences, 270 (2003), pp. 2565–2571.
- 720 [10] N. FERGUSON, D. LAYDON, G. NEDJATI GILANI, N. IMAI, K. AINSLIE, M. BAGUELIN, S. BHATIA,
 721 A. BOONYASIRI, Z. CUCUNUBA PEREZ, G. CUOMO-DANNENBURG, ET AL., *Report 9: Impact*
 722 *of non-pharmaceutical interventions (npis) to reduce covid19 mortality and healthcare de-*
 723 *mand*, (2020).
- 724 [11] N. M. FERGUSON, D. A. CUMMINGS, C. FRASER, J. C. CAJKA, P. C. COOLEY, AND D. S.
 725 BURKE, *Strategies for mitigating an influenza pandemic*, Nature, 442 (2006), pp. 448–452.
- 726 [12] M. FITZGERALD, D. THIRLBY, AND C. BEDFORD, *The outcome of contact tracing for gonorrhoea*
 727 *in the united kingdom*, International journal of STD & AIDS, 9 (1998), pp. 657–660.
- 728 [13] C. FOIAS, A. TANNENBAUM, AND G. ZAMES, *Weighted sensitivity minimization for delay sys-*
 729 *tems*, IEEE Transactions on Automatic Control, 31 (1986), pp. 763–766.
- 730 [14] C. FRASER, S. RILEY, R. M. ANDERSON, AND N. M. FERGUSON, *Factors that make an infectious*
 731 *disease outbreak controllable*, Proceedings of the National Academy of Sciences, 101 (2004),
 732 pp. 6146–6151.
- 733 [15] J. HASELL, E. MATHIEU, D. BELTEKIAN, B. MACDONALD, C. GIATTINO, E. ORTIZ-OSPINA,
 734 M. ROSER, AND H. RITCHIE, *A cross-country database of covid-19 testing*, Scientific data,
 735 7 (2020), pp. 1–7.
- 736 [16] W. O. KERMACK AND A. G. MCKENDRICK, *A contribution to the mathematical theory of*
 737 *epidemics*, Proceedings of the royal society of london. Series A, Containing papers of a
 738 mathematical and physical character, 115 (1927), pp. 700–721.
- 739 [17] P. KHARGONEKAR AND A. TANNENBAUM, *Non-euclidian metrics and the robust stabilization of*
 740 *systems with parameter uncertainty*, IEEE Transactions on Automatic Control, 30 (1985),
 741 pp. 1005–1013, <https://doi.org/10.1109/TAC.1985.1103805>.
- 742 [18] I. Z. KISS, D. M. GREEN, AND R. R. KAO, *The effect of network mixing patterns on epidemic*
 743 *dynamics and the efficacy of disease contact tracing*, Journal of the Royal Society Interface,
 744 5 (2008), pp. 791–799.
- 745 [19] B. A. MACKE AND J. E. MAHER, *Partner notification in the united states: an evidence-based*
 746 *review*, American Journal of Preventive Medicine, 17 (1999), pp. 230–242.
- 747 [20] J. MÜLLER AND B. KOOPMANN, *The effect of delay on contact tracing*, Mathematical bio-
 748 sciences, 282 (2016), pp. 204–214.
- 749 [21] J. MÜLLER, M. KRETZSCHMAR, AND K. DIETZ, *Contact tracing in stochastic and deterministic*
 750 *epidemic models*, Mathematical biosciences, 164 (2000), pp. 39–64.
- 751 [22] M. NUNO, C. CASTILLO-CHAVEZ, Z. FENG, AND M. MARTCHEVA, *Mathematical models of in-*

752 *fluenza: the role of cross-immunity, quarantine and age-structure*, in Mathematical Epi-
 753 demiology, Springer, 2008, pp. 349–364.
 754 [23] Y. J. PARK, Y. J. CHOE, O. PARK, S. Y. PARK, Y.-M. KIM, J. KIM, S. KWEON, Y. WOO,
 755 J. GWACK, S. S. KIM, ET AL., *Contact tracing during coronavirus disease outbreak, south*
 756 *korea, 2020*, Emerging infectious diseases, 26 (2020), pp. 2465–2468.
 757 [24] G. STEIN, *Respect the unstable*, IEEE Control Systems Magazine, 23 (2003), pp. 12–25.

758 **Appendix A. Proof of Theorem 2.1.**

759 Eliminating S using the algebraic equation in (2.4) and then linearising about the
 760 point $(I, R, Q) = (0, 0, 0)$ shows that for small deviations,

761 (A.1)
$$\frac{d}{dt} \begin{bmatrix} I \\ R \end{bmatrix} = \begin{bmatrix} \beta - \gamma & 0 \\ 0 & -\gamma \end{bmatrix} \begin{bmatrix} I \\ R \end{bmatrix} - \begin{bmatrix} \beta \\ 0 \end{bmatrix} Q.$$

762 Equation (2.5) is already linear. We are therefore required to show that the in-
 763 terconnection of (A.1) and (2.5) is stable. The equation in R is decoupled and
 764 stable, so can be safely ignored. It is convenient to introduce the transfer func-
 765 tions $\mathbf{G}_1 = -\beta/(s - \beta + \gamma)$ and $\mathbf{G}_2 = \alpha \exp(-\gamma T_{\text{delay}}) \exp(-s T_{\text{delay}})$. These are the
 766 transfer functions from Q to I in (A.1) and from I to Q in (2.5) respectively. Since \mathbf{G}_1
 767 is unstable, we are therefore required to show that $\mathbf{G}_1 (1 - \mathbf{G}_1 \mathbf{G}_2)^{-1}$ is stable. This
 768 is equivalent to the saying that the denominator of this transfer function has no poles
 769 in the closed right-half-plane. For the transfer functions in question, the condition is
 770 that:

771
$$s + \gamma + \alpha\beta \exp(-\gamma T_{\text{delay}}) \exp(-s T_{\text{delay}}) - \beta \neq 0, \forall s \in \overline{\mathbb{C}}_+.$$

772 Putting $\tilde{s} = s/\beta$ and rearranging shows that this is equivalent to

773
$$\tilde{s} + R_0^{-1} + \alpha \exp(-\beta T_{\text{delay}} (\tilde{s} + R_0^{-1})) \neq 1, \forall \tilde{s} \in \overline{\mathbb{C}}_+.$$

774 A standard Nyquist argument then shows that this holds if and only if the curve
 775 $f(\tilde{s}) := \tilde{s} + R_0^{-1} + \alpha \exp(-\beta T_{\text{delay}} (\tilde{s} + R_0^{-1}))$ when evaluated along the usual Nyquist
 776 D -contour does not encircle 1. A simple sufficient condition for this is that

- 777 (i) $f(0) > 1$;
 778 (ii) $\frac{d}{d\omega} (\text{Im}(f(j\omega))) > 0$;

779 since together (i)–(ii) ensure that the curve only crosses the real axis to the right of 1
 780 (technically we also need $\lim_{x \rightarrow \infty} f(x) > 1$, but this is trivially satisfied by our f). It
 781 is readily checked that (i) is equivalent to the condition from the theorem statement.
 782 That is

783 (A.2) (i) $\iff T_{\text{delay}} < \frac{1}{\gamma} \ln \left(\frac{\alpha}{1 - R_0^{-1}} \right).$

784 For (ii), observe that

785
$$\frac{d}{d\omega} (\text{Im}(f(j\omega))) = 1 - \alpha\beta T_{\text{delay}} \exp(-\beta T_{\text{delay}} R_0^{-1}) \cos(\beta T_{\text{delay}} \omega).$$

786 Therefore it is sufficient that $\alpha\beta T_{\text{delay}} \exp(-\beta T_{\text{delay}} R_0^{-1}) < 1$. We will demonstrate
 787 this in two stages. First observe that $\alpha\beta T_{\text{delay}} \exp(-\beta T_{\text{delay}} R_0^{-1}) \leq \alpha R_0 \exp(-1)$.
 788 Therefore if $R_0 \leq \exp(1)$, (ii) holds (recall that $0 \leq \alpha \leq 1$). Now assume that
 789 $R_0 > \exp(1)$. We then see that if this is the case

790 (A.3)
$$\ln \left(\frac{\alpha}{1 - R_0^{-1}} \right) \leq \ln \left(\frac{1}{1 - \exp(-1)} \right) \approx 0.5 \leq 1.$$

791 Next observe that for $x \leq R_0$, the function $x \exp(-x/R_0)$ is monotonically increasing
 792 in x . Therefore given any $T \geq T_{\text{delay}}$, if $\beta T \leq R_0$, then

$$793 \quad (\text{A.4}) \quad \alpha \beta T_{\text{delay}} \exp(-\beta T_{\text{delay}} R_0^{-1}) \leq \alpha \beta T \exp(-\beta T R_0^{-1}).$$

794 Now define

$$795 \quad T^* = \frac{1}{\gamma} \ln \left(\frac{\alpha}{1 - R_0^{-1}} \right).$$

796 By (A.3), $\beta T^* \leq R_0$. Furthermore

$$797 \quad \alpha \beta T^* \exp(-\beta T^* R_0^{-1}) = R_0 (1 - R_0^{-1}) \ln \left(\frac{\alpha}{1 - R_0^{-1}} \right) \leq 1.$$

798 Therefore by (A.4), (ii) holds for any $T_{\text{delay}} \leq T^*$. However by (A.2), (i) $\implies T_{\text{delay}} <$
 799 T^* . So (i) \implies (ii) and (i) is sufficient for stability. Necessity follows since increasing
 800 T_{delay} causes $f(1) = 1$ indicating a change in the winding number, and hence the
 801 onset of instability.

802 **Appendix B. Extending Theorem 2.2 to the Nonlinear Setting.**

803 In this section we will demonstrate that under appropriate assumptions, a natural
 804 analogue of Theorem 2.2 holds in the nonlinear setting. To do this we will prove that
 805 the induced \mathcal{L}_2 -norm of a system is always lower-bounded by the induced \mathcal{L}_2 -norm
 806 of its linearisation. Since the induced \mathcal{L}_2 -norm of an LTI system is equal to its H-
 807 infinity norm, this shows that if the linearisation of a nonlinear system is LTI, then
 808 the induced \mathcal{L}_2 -norm of the sensitivity function of the nonlinear system must satisfy
 809 the same bound from Theorem 2.2.

810 The result we are trying to prove is in fact rather elementary. However it requires
 811 a bit of set up to lay out the appropriate definitions and concepts. The difficulties
 812 stem from the fact that we would like to combine nonlinear state-space models (to
 813 describe general compartmental models for disease spread) and delays. Accordingly
 814 we adopt the standard operator theoretic set up on \mathcal{L}_2 which covers both these types
 815 of model. More specifically, \mathcal{L}_2 is the space of functions $f : [0, \infty) \rightarrow \mathbb{R}$ with finite
 816 norm

$$817 \quad \|f\| := \sqrt{\int_0^\infty |f(t)|^2 dt}.$$

818 This is a subspace of \mathcal{L}_{2e} , who's members need only be square integrable on finite
 819 intervals. An operator is a function $\mathcal{G} : \mathcal{L}_{2e} \rightarrow \mathcal{L}_{2e}$, and the induced \mathcal{L}_2 -norm of an
 820 operator is defined as

$$821 \quad \|\mathcal{G}\|_{\mathcal{L}_2} := \sup \left\{ \frac{\|\mathcal{G}(u)\|}{\|u\|} : u \in \mathcal{L}_{2e}, u \neq 0 \right\}.$$

822 In the case that the operator \mathcal{G} is describing the dynamics of a LTI system with
 823 transfer function \mathbf{G} , $\|\mathcal{G}\|_{\mathcal{L}_2} = \|\mathbf{G}\|_\infty$.

824 The natural generalisation of a linearisation in this setting is given by the Fréchet
 825 derivative. An operator \mathcal{G} is Fréchet differentiable at a point $x \in \mathcal{L}_2$ if there exists a
 826 linear operator \mathcal{A} such that

$$827 \quad \lim_{h \rightarrow 0} \frac{\|\mathcal{G}(x+h) - \mathcal{G}(x) - \mathcal{A}(h)\|}{\|h\|} = 0.$$

828 If such a linear operator exists, it is unique, and we denote the Fréchet derivative of
 829 \mathcal{G} at x as $D\mathcal{G}(x) = \mathcal{A}$.

830 With these definitions in place, we are ready to state the main result of this sec-
 831 tion. The following lemma shows that provided the linearisation exists, the induced
 832 \mathcal{L}_2 -norm of the linearisation of an operator about a fixed point (an equilibrium point)
 833 is always smaller than the \mathcal{L}_2 -norm of the operator itself. This means that if we have
 834 a nonlinear system \mathcal{G} with linearisation described by an **LTI** system with transfer func-
 835 tion \mathbf{G} , then $\|\mathcal{G}\|_{\mathcal{L}_2} \geq \|\mathbf{G}\|_{\infty}$. This immediately gives us a nonlinear generalisation of
 836 **Theorem 2.2**. In particular if we instead study the nonlinear feedback interconnection

$$837 \quad (B.1) \quad \begin{aligned} e_i &= \mathcal{G}_i(e_{i-1}) + d_i, \quad i \in \{1, \dots, n\} \\ e_0 &= -e_n, \end{aligned}$$

838 and define the sensitivity functions to be the operators $\mathcal{S}_i : d_i \rightarrow e_i$, then provided the
 839 linearisations of \mathcal{S}_i are **LTI**, then $\|\mathcal{S}_i\|_{\mathcal{L}_2}$ must satisfy exactly the same lower bound
 840 from **Theorem 2.2**.

841 **LEMMA B.1.** *Given an operator \mathcal{G} , if $\mathcal{G}(0) = 0$ and \mathcal{G} is Fréchet differentiable at*
 842 *0, then*

$$843 \quad \|\mathcal{G}\|_{\mathcal{L}_2} \geq \|D\mathcal{G}(0)\|_{\mathcal{L}_2}.$$

844 *Proof.* Let $\mathcal{A} = D\mathcal{G}(0)$. Using the reverse triangle inequality shows that for any
 845 non-zero $x \in \mathcal{L}_{2e}$ and non-zero $\epsilon \in \mathbb{R}$,

$$846 \quad \begin{aligned} \|\mathcal{G}\|_{\mathcal{L}_2} &\geq \|\mathcal{G}(\epsilon x)\| / \|\epsilon x\| = \|\mathcal{G}(\epsilon x) - \mathcal{A}(\epsilon x) + \mathcal{A}(\epsilon x)\| / \|\epsilon x\| \\ &\geq \|\mathcal{A}(x)\| / \|x\| - \|\mathcal{G}(\epsilon x) - \mathcal{A}(\epsilon x)\| / \|\epsilon x\|. \end{aligned}$$

847 Taking the limit $\epsilon \rightarrow 0$, we see from the definition of the Fréchet derivative that this
 848 implies that $\|\mathcal{G}\|_{\mathcal{L}_2} \geq \|\mathcal{A}(x)\| / \|x\|$. Taking the sup over $x \in \mathcal{L}_{2e}$ gives the result. \square